GLOBAL FITS TO RADIATIVE $b \to s$ TRANSITIONS

S. DESCOTES-GENON

Laboratoire de Physique Théorique (CNRS/Univ. Paris-Sud, UMR 8627), 91405 Orsay, France

I review the status of the model-independent analyses of $b \to s$ transitions. I discuss first the effective Hamiltonian approach, before focusing on the impact of $B \to K^*\ell\ell$ and $B \to K\ell\ell$ observables. I consider several global fits performed recently, discussing some of their differences. Finally, I give a brief overview of some limitations and prospects for theoretical and experimental improvement.

1 Radiative $b \to s$ transitions in a model-independent approach

Radiative $b \to s\gamma$ and $b \to s\ell\ell$ transitions are particularly interesting flavour processes. These Flavour-Changing Neutral Currents are suppressed in the Standard Model (SM) and dominated by loop processes involving only heavy particles (top, W, Z). As such, they are expected to be particularly sensitive probes of New Physics (NP) occurring at higher energies. This explains the experimental interest in measuring these processes, at Babar, Belle, CDF, DØ, and currently at LHCb and CMS. If these measurements can be analysed in particular scenarios of New Physics (Z' boson, composite models, supersymmetry, extra-dimensions...), the presence of very different scales for the external states (at most $O(m_b)$) and the internal degrees of freedom ($O(M_W)$ or above) allows for model-independent analyses relying on the effective Hamiltonian approach. The latter is obtained by focusing on $b \to s$ transitions and integrating out all heavy degrees of freedom, leading to the following Hamiltonian (in the case of the SM):

$$\mathcal{H}^{SM}_{\Delta F=1} = -\frac{4G_F}{\sqrt{2}}\left\{V_{tb}V_{ts}^*\left[\mathcal{C}_1 Q_1^c + \mathcal{C}_2 Q_2^c + \sum_{i=3\ldots10}\mathcal{C}_i Q_i\right] + V_{tu}V_{us}^*[\mathcal{C}_1(Q_1^c - Q_1^u) + \mathcal{C}_2(Q_2^c - Q_2^u)]\right\} \tag{1}$$

up to contributions suppressed by additional powers of m_b/M_W. The Wilson coefficients $\mathcal{C}_i$ describe the short-distance physics (function of $m_t, m_W \ldots$ in the SM) whereas the local operators Q_i correspond to long-distance physics involving only light/soft degrees of freedom. In this framework, $b \to s$ transitions are mainly described by $Q_7 = e/(4\pi)^2 \bar{s}\sigma^{\mu\nu}(1+\gamma_5)F_{\mu\nu}\, b$, related to the emission of a real or soft photon, $Q_9 = e^2/(4\pi)^2\bar{s}\gamma_\mu(1-\gamma_5)b\ \bar{\ell}\gamma_\mu\ell$ involved in $b \to s\mu\mu$ via the emission of a Z boson or a hard photon, and $Q_{10} = e^2/(4\pi)^2\bar{s}\gamma_\mu(1-\gamma_5)b\ \bar{\ell}\gamma_\mu\gamma_5\ell$ involved in $b \to s\mu\mu$ via the emission of a Z boson. The value of the Wilson coefficients can be obtained by matching the SM at a high-energy scale $\mu_0 = O(m_t)$ and evolving down at $\mu_{\rm ref} = O(m_b)$ [typically 4.8 GeV, with typical values $\mathcal{C}_7^{SM} = -0.29$, $\mathcal{C}_9^{SM} = 4.1$, $\mathcal{C}_{10}^{SM} = -4.3$ (the matching and running formulae are known up to NNLO, including electromagnetic corrections). In the SM, there are additional contributions to the decay coming from 4-quark operators, in particular from the effective operator $Q_1^c = [\bar{s}\gamma_\mu(1-\gamma_5)c][\bar{c}\gamma_\mu(1-\gamma_5)b]$ (corresponding to a W exchange) where the $c\bar{c}$ loop closes to emit a virtual photon yielding a di-lepton pair. The leading effect coming from such four-quark operators can be absorbed in $\mathcal{C}_9^{\rm eff} = \mathcal{C}_9 + Y(q^2)$.

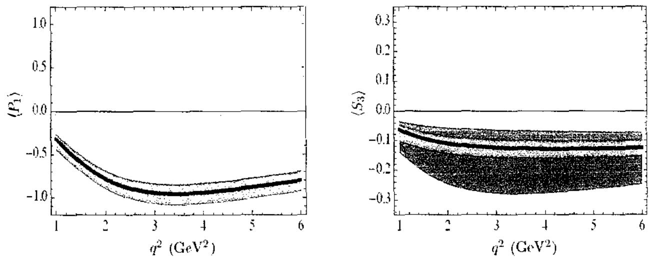

Figure 1 – Predictions for the form-factor sensitive observable S_3 and form-factor independent observable P_1: binned predictions in the SM (yellow) and predictions for a NP benchmark point (affecting $\mathcal{C}_{7,7',9,10}$), with two different types of hadronic inputs (green [6] and grey [7]) [8].

The presence of New Physics can modify this picture by modifying the value of the Wilson coefficients $\mathcal{C}_{7,9,10}$, but also by allowing new long-distance operators Q_i, which would be very suppressed or absent in the Standard Model. This yields the chirally-flipped operators $Q_{7',9',10'}$ (obtained for instance by the presence of a W' coupling to right-handed fermions), scalar and pseudoscalar operators $Q_{S,S',P,P'}$ (induced e.g., by the exchange of charged scalar or pseudoscalar Higgs-like bosons) or tensor operators $Q_{T,T'}$ (allowed in principle, but difficult to generate in viable models). These NP contributions are expressed as $\mathcal{C}_i = \mathcal{C}_i^{SM} + \mathcal{C}_i^{\rm NP}$ at $\mu_{\rm ref}$.

Combining measurements on inclusive and exclusive $b \to s\gamma(^*)$ processes allows one to constrain the values of the different Wilson coefficients, as long as one has experimental measurements and theoretical input for long-distance (hadronic) physics. Several groups have performed such analyses within different approaches, in some cases providing also NP interpretations of their results [1,2,3,4]. One should emphasise that several modes have been of particular interest recently, namely the inclusive $B \to X_s\gamma$ branching ratio predicted with a high accuracy in the SM, the exclusive $B_s \to \mu\mu$ measured with increased accuracy at LHCb and CMS, with recent theoretical progress on higher-order QCD and electroweak corrections, the inclusive $B \to X_s\ell\ell$ branching ratio recently measured by Babar in several bins, the exclusive $B \to K\ell\ell$ measured with very fine binning by LHCb, and the exclusive $B \to K^*\ell\ell$ decays measured by LHCb, showing interesting departures from the SM. Since most of the modes have been covered by other presentations of this conference [5], I will focus on the last item, which has a deep impact on the outcome of global fits to radiative $b \to s$ Wilson coefficients.

2 $B \to K^*\ell\ell$

The $B \to K^*\ell\ell$ decay with a subsequent decay of $K^* \to K\pi$ has a complicated kinematic structure [9]. The differential branching decay ratio can be described in terms of 12 angular coefficients I_j, which correspond to interferences between 8 transversity amplitudes, indexed according to the polarisation $(\perp, ||, 0, t)$ of the (real) K^* meson and the (virtual) intermediate boson $V^* = \gamma^*, Z^*$ (or scalar) as well as the chirality (L, R) of $\mu^+\mu^-$ pair. In a first approximation, these amplitudes $A_{\perp,L/R}$, $A_{||,L/R}$, $A_{0,L/R}$, A_t (together with the scalar amplitude A_s) depend on the dilepton invariant mass square $q^2 = s$, the Wilson coefficients $\mathcal{C}_7, \mathcal{C}_9, \mathcal{C}_{10}, \mathcal{C}_S, \mathcal{C}_P$ (and their flipped-chirality counterparts) as well as $B \to K^*$ form factors $A_{0,1,2}$, V, $T_{1,2,3}$ from the matrix elements $\langle K^*|Q_i|B\rangle$ of the effective Hamiltonian.

There are four different regions for the analysis of the decay. At very large K^*-recoil ($4m_\ell^2 < q^2 < 1$ GeV^2), the photon is almost real, and one is sensitive to its pole via a $\mathcal{C}_7/q^2$ divergence, together with the presence of light resonances (ρ, ϕ). At large K^*-recoil ($q^2 < 9$ GeV^2), the K^* is energetic ($E_{K^*} \gg \Lambda_{QCD}$) and $B \to K^*$ form factors can be estimated using light-cone sum rules (LCSR). In the charmonium region ($q^2 = m^2_{\psi,\psi'...}$ between 9 and 14 GeV^2), predictions are very

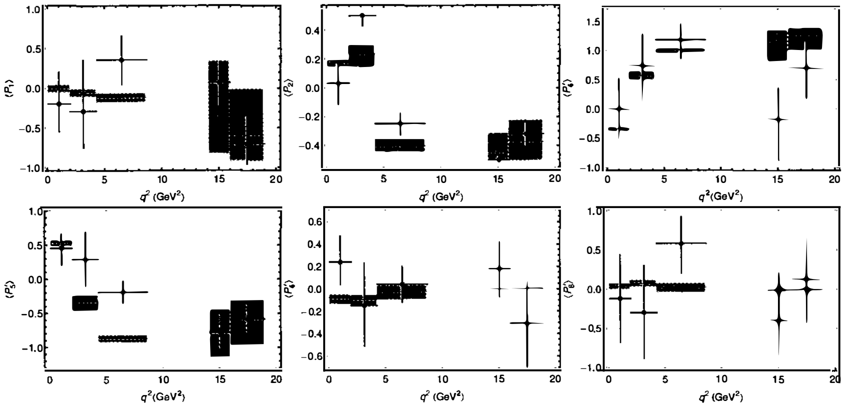

Figure 2 – Form-factor independent observables for $B \to K^*\ell$ (at low-recoil). Crosses indicate LHCb results, blue curves are the SM predictions, purple boxes their binned counterparts.)

difficult due to the lack of precise description of the $c\bar{c}$ resonances which interfere significantly in this region. At low K^*-recoil ($q^2 > 14$ GeV^2), the K^* meson is soft ($E_{K^*} \simeq \Lambda_{QCD}$), and the form factors can be derived using lattice QCD simulations. In this region, there are further charmonium resonances, but it is expected that the quark-hadron duality holds for sufficiently inclusive quantities, at an accuracy still under discussion. On the other hand, in the large K^* region, one may expect the region $q^2 \geq 6$ GeV^2 to be already affected by the tail of the J/ψ resonance. The presence of two regions of large- and low-K^* recoils where E_{K^*} is of order M_B or Λ_{QCD} is particularly interesting from the theoretical point of view, as effective theories can be built in both cases, respectively Soft-Collinear Effective Theory (boiling down to QCD factorisation in this particular setting) and Heavy-Quark Effective Theory. These effective theories disentangle soft $[O(\Lambda_{QCD}]$ from hard physics $[O(m_B)]$ in particular quantities. In the limit $m_b \to \infty$, the soft physics embedded in the 7 $B \to K^*$ form factors boil down to 2 soft form factors $\xi_\perp(q^2)$ and $\xi_{||}(q^2)$ in the large K^*-recoil limit [9], and 3 soft form factors $f_\perp(q^2), f_{||}(q^2), f_0(q^2)$ in the low K^*-recoil limit [10]. In both cases, the relationships between full form factors and soft form factors get corrected by $O(\alpha_s)$ corrections from hard gluons (which can be computed within perturbation theory) and $O(\Lambda/m_B)$ non-perturbative corrections (which can only be estimated).

These simplifications have triggered the development of observables which are expected to exhibit little sensitivity to form factors at low- and/or large-K^* recoils. In the massless lepton limit and in the absence of scalar contributions, one can show that 8 independent observables can be built in the large-recoil region: 6 can be chosen to be form factor-independent ($P_{1,2,3}$ and $P'_{4,5,6}$), and 2 other must be form-factor dependent (for instance the decay rate Γ or the longitudinal fraction F_L) [11]. A similar analysis can be made at low recoil [12]. Such observables are independent of hadronic form factors at leading order in the $1/m_b$ expansion for the kinematic range of interest, but keep a residual form-factor dependence once the corrections to the heavy-quark limit are included. This dependence is however much smaller than in the case of ordinary observables, and makes these observables particularly well suited to pin down NP contributions, as the results will affected only marginally by hadronic effects. This is illustrated in Fig. 1 for the two observables S_3 (CP-averaged version of the angular coefficient I_3) and $P_1 = 2S_3/(1 - F_L)$, in the Standard Model and in a particular scenario of NP affecting $\mathcal{C}_{7,7',9,10}$. Two different sets hadronic form factors are used in the latter case, obtained from the LCSR [6,7]. As some of these determination have substantial uncertainties, it is not really surprising that the form-factor observable S_3 exhibit so large errors that they prevent from discriminating between the SM case and the NP point considered. On the other hand, both sets of form factors yield the same result for the form-factor independent P_1, which remain a good probe of NP for both choices of hadronic inputs.

LHCb has recently presented [13] binned results for $B \to K^*\ell\ell$ form-factor independent observables at large recoil, for $q^2 \in [0.1, 2], [2, 4.3], [4.3, 8.68]$ GeV^2, as well as a wide bin [1,6] GeV^2, and at low recoil for $q^2 \in [14.18, 16], [16, 19]$ GeV^2. The results show an interesting pattern of deviations with respect to the Standard Model in P_2 [with $2.9\,\sigma$ (1.7σ) deviation in the second (third) bin] and P_5' [$4.3\,\sigma$ (1.6σ) deviation on the third (second) bin]. P_2 has the same zero as A_{FB}, related to $\mathcal{C}_9/\mathcal{C}_7$, whereas $P_5' \to -1$ as q^2 grows, due to the smallness of $A^R_{\perp,||}$ compared to $A^L_{\perp,||}$ for the SM values $\mathcal{C}_9^{SM} \simeq -\mathcal{C}_{10}^{SM}$, so that both deviations could be accommodated by taking $\mathcal{C}_9$ smaller than its SM value.

3 A first global analysis

3.1 General framework

This result can be confirmed through a global analysis of $b \to s$ transitions. A first analysis of radiative decays was presented [1], considering the following observables:

- *Optimised observables in $B \to K^*\mu^+\mu^-$*: P_1, P_2, P_4', P_5', P_6' and P_8', within the 3 large-recoil bins [0.1,2], [2,4.3] and [4.3,8.68] GeV^2, and the 2 low-recoil bins [14.18,16] and [16,19] GeV^2.

- *Forward-Backward Asymmetry in $B \to K^*\mu^+\mu^-$*: Once one has chosen a maximal set of optimised observables, one has still to choose two independent observables sensitive to form-factor uncertainties. The differential branching ratio dBr/dq^2 is one of them, necessary to fix the overall normalization. $A_{\rm FB}$ was chosen because of its expected higher sensitivity to $\mathcal{C}_9^{\rm NP}$ and its complementarity with P_2 [9].

- *Radiative and dileptonic B decays*: Other important $b \to s$ penguin modes sensitive to magnetic and dileptonic operator were considered:the branching ratios $\mathcal{B}(B \to X_s\gamma)_{E_\gamma > 1.6\rm GeV}$, $\mathcal{B}(B \to X_s\mu^+\mu^-)_{[1,6]}$ and $\mathcal{B}(B_s \to \mu^+\mu^-)$, the isospin asymmetry $A_I(B \to K^*\gamma)$ and the $B \to K^*\gamma$ time-dependent CP asymmetry $S_{K^*\gamma}$. Other similar observables were disregarded, either because their theoretical description is not ascertained, such as $A_{CP}(B \to X_s\gamma)$, or because of experimental issues, as is the case with $B \to K\mu^+\mu^-$ at the time of the analysis.

For $B \to K^*\mu\mu$, only the LHCb measurements have been considered. QCD factorisation was used to compute large-recoil observables, with soft form factors determined from the LCSR estimates of full form factors [7]. The considerations of the pulls for the various NP hypotheses shows that the full set of large- and low-recoil data for $B \to K^*\mu^+\mu^-$ obtain the larger pulls (around $\sim 4\,\sigma$) when adding $\mathcal{C}_9^{\rm NP}$, independently of which other Wilson coefficients are left free to receive NP contributions. The next-to-larger pulls are obtained by adding $\mathcal{C}_7^{\rm NP}$ (around $\sim 3\,\sigma$), in all cases except when $\mathcal{C}_9^{\rm NP}$ has been added beforehand; in such a case, the pull is $\sim 1.3\,\sigma$ (still the largest after $\mathcal{C}_9^{\rm NP}$). The rest of the pulls are always around or below $1\,\sigma$. These results are consistent with the fact that $\mathcal{C}_9$ plays a prominent role in explaining the $B \to K^*\mu^+\mu^-$ anomaly; besides that, a NP contribution to $\mathcal{C}_7$ is also favoured due to $B \to X_s\gamma$ though less strongly. If only the large-recoil bins are considered, the main picture remains the same, although in some cases some other coefficients may play a (more modest) role in the discussion. Finally, using both low- and large-recoil data for $B \to K^*\mu^+\mu^-$, one can compute the pull corresponding to the $\mathcal{C}^{\rm NP}_{10,7',9',10'} = 0$ hypothesis in the scenario where all 6 Wilson coefficients are allowed to receive NP contributions. The resulting pull is below the $\sim 0.1\,\sigma$ level, indicating that no other

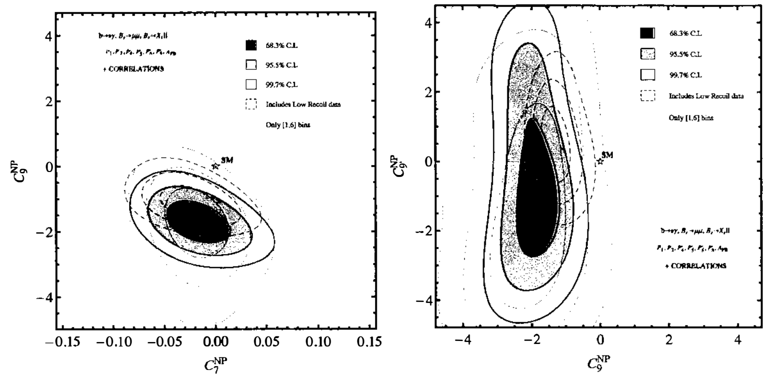

Figure 3 – Fit in the $(\mathcal{C}_7^{\rm NP}, \mathcal{C}_9^{\rm NP})$ (left) and $(\mathcal{C}_9^{\rm NP}, \mathcal{C}_{9'}^{\rm NP})$ (right) hypotheses, using the three large-recoil bins for $B \to K^*\mu^+\mu^-$ observables, together with $B \to X_s\gamma$, $B \to X_s\mu^+\mu^-$, $B \to K^*\gamma$ and $B_s \to \mu^+\mu^-$. The dashed contours include both large- and low-recoil bins, whereas the orange ones use only the 1-6 GeV^2 bin for $B \to K^*\mu^+\mu^-$ observables. The SM star $\mathcal{C}_{7,9}^{\rm NP} = (0,0)$ point corresponds to $\mathcal{C}_{7,9}^{\rm SM} = (-0.29, 4.07)$ at $\mu_b = 4.8$ GeV. Experimental correlations are included [1].

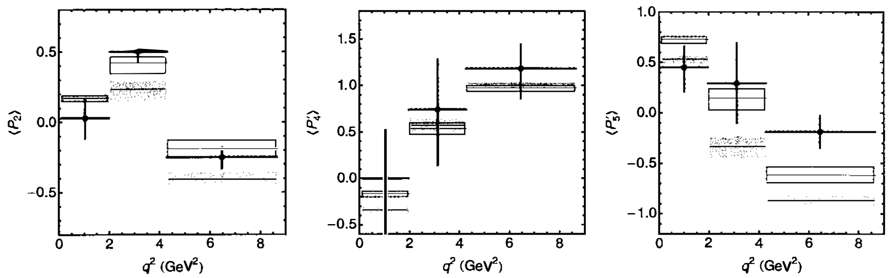

Figure 4 – Comparison between the SM predictions (gray boxes), the experimental measurements (blue data points) and the predictions for the scenario with $\mathcal{C}_9^{\rm NP} = -1.5$ and other $\mathcal{C}_i^{\rm NP} = 0$ (red squares) [1].

NP contribution is required by the data apart from $\mathcal{C}_9^{\rm NP}$ and $\mathcal{C}_7^{\rm NP}$. The same results occur when only large-recoil data is used.

3.2 2D scenarios

Let us focus now on the implications for New Physics in $\mathcal{C}_7$ and $\mathcal{C}_9$. A standard χ^2 fit to $\mathcal{C}_7^{\rm NP}$, $\mathcal{C}_9^{\rm NP}$ was performed [14,1], taking only the first three large-recoil bins for $B \to K^*\mu^+\mu^-$. The result is shown in the left-hand panel of Fig. 3, where 68.3% (red), 95.5% (green), and 99.7% (yellow) C.L. regions are shown. The best fit point is obtained for $\mathcal{C}_9^{\rm NP} \sim -1.5$ and $\mathcal{C}_7^{\rm NP} \sim -0.03$. In this scenario, the SM hypothesis $\mathcal{C}_7^{\rm NP} = 0, \mathcal{C}_9^{\rm NP} = 0$ has a pull of $4.2\,\sigma$. Including the low-recoil bins decreases slightly the significance of the effect, since these observables are less constraining and compatible with the SM currently. The corresponding regions are indicated by the dashed curves in Fig. 3. The inclusion of the low-recoil data reduces the discrepancy with respect to the SM to $3.5\,\sigma$. In both cases, P_2 and P_5' drive the fits away from the SM point.

One can repeat the analysis taking the input for the $B \to K^*\mu^+\mu^-$ observables to $[1,6]$ GeV^2 bins, exploiting several theoretical and experimental advantages. Such wider bins collect more events with larger statistics. Furthermore, some theoretical issues are less acute, such as the effect of low-mass resonances at very low $q^2 \ll 1$ GeV^2 [18], or the impact of charm loops above ~ 6 GeV^2 [7]. On the other hand, integrating over such a large bin washes out some effects

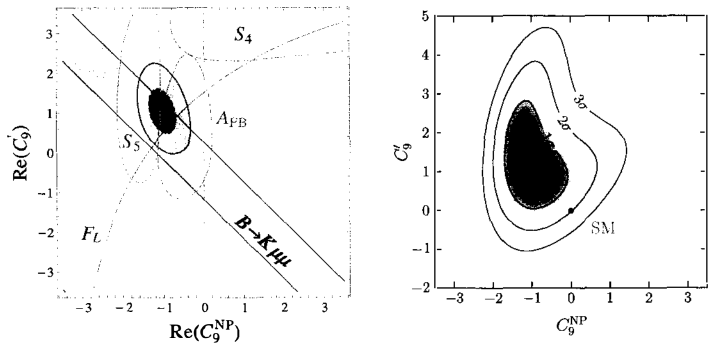

Figure 5 – Global analyses of $b \to s$ transitions from a frequentist analysis of non-optimised $B \to K^*\ell\ell$ observables together with other radiative observables (left-hand panel) [2] and from the fit to $B \to K^*\mu\mu$ and $B_s \to \phi\mu\mu$ observables exploiting lattice computations of the form factors at low recoil (right-hand panel) [4].

related to the q^2 dependence of the observables, so that this analysis should have less sensitivity to NP [8]. This can be seen in Fig. 3, where the regions in this case are indicated by the orange curves, and, as expected, the constraints get slightly weaker. In addition, due to the fact that theoretical uncertainties happen to increase moderately for large negative NP contributions to $\mathcal{C}_9$, the constraints are more relaxed in the lower region of the $\mathcal{C}_7^{\rm NP} - \mathcal{C}_9^{\rm NP}$ plane. Even in this rather conservative situation the main conclusion (a NP contribution $\mathcal{C}_9^{\rm NP} \sim -1.5$) still prevails, whereas the SM hypothesis has still a pull of 3.3 σ.

A comment is in order concerning alternative scenarios with different sets of coefficients receiving NP contributions. In all scenarios considered [1] the best fit corresponds to $\mathcal{C}_9^{\rm NP} \sim -1.2$ with a significant preference for negative values. In addition, a slight preference of negative values of $\mathcal{C}_{9'}^{\rm NP}$ or $\mathcal{C}_7^{\rm NP}$ occurs (with much less significance). It arises for $\mathcal{C}_{9'}^{\rm NP}$ only when only large-recoil data is considered: $\mathcal{C}_{9'}^{\rm NP} < 0$ is favoured to raise the value of $\langle P_5' \rangle_{[4.3,8.48]}$ without spoiling the agreement between theory and experiment in the first bin. This possibility is however weakened by the low-recoil data. This is illustrated in the right-hand panel of Fig. 3.

4 Subsequent analyses

Another frequentist analysis has been performed [2], along similar lines. As far as the inputs are concerned, the main differences concern the use of only the wide [1,6] bin, the inclusion of $Br(B \to K\ell\ell)$, the average over all experiments (and not only LHCb), a choice of non-optimised $B \to K^*\ell\ell$ observables, and a different approach for the computation of $B \to K^*\ell\ell$ amplitudes (complementing full form factors with non-factorisable corrections, rather than relying on QCD factorisation). There is a preference for $\mathcal{C}_9^{\rm NP} \simeq -0.9$, however with a lesser significance due to the use of non-optimised observables and wide bins for $B \to K^*\ell\ell$ observables. At the time of the analysis, the value of $Br(B \to K\mu\mu)$ at low-recoil was in good agreement with the SM expectations, requiring a contribution $\mathcal{C}_{9'}^{\rm NP} > 0$ to cancel that of $\mathcal{C}_9^{\rm NP}$ to this observable, as illustrated on the left-hand panel of Fig. 5.

A Bayesian analysis has also been performed [3]. Once again, only wide [1-6] bins are used for $B \to K^*\ell\ell$. The Bayesian approach requires to impose priors on nuisance parameters (values of the form factors, power-suppressed corrections). The analysis seems to yield reasonable agreement with the SM if Λ/m_b corrections are allowed to shift by 10 to 20% (even though the interpretation of the goodness-of-fit from $\chi^2_{\rm min}$ is rather delicate far from the asymptotic limit and would require a dedicated study of the appropriate N_{dof}). On the other hand, the consideration of the Bayes factor favour NP in both SM operators and chirally flipped operators, whether in the generic case or restricted to $\mathcal{C}_9$ and $\mathcal{C}_{9'}$.

Lattice simulations are now focusing on these decays in the low-K^* recoil region [4]. The $B \to K^*\ell\ell$ and $B_s \to \phi\ell\ell$ form factors have been computed using NRQCD and staggered quarks, with the interesting result that there is a disagreement between the SM predictions and the measurement of both branching ratios at low recoil. A frequentist fit on only low-recoil data on $B \to K^*\mu\mu$ and $B_s \to \phi\mu\mu$ favours $\mathcal{C}_9^{\rm NP} < 0$ (and $\mathcal{C}_{9'}^{\rm NP} > 0$ if both low-recoil bins are considered), as illustrated on the right-hand panel of Fig. 5.

It is interesting to notice that all analyses agree with an NP contribution $\mathcal{C}_9^{\rm NP} < 0$, but disagree on the need for $\mathcal{C}_{9'}^{\rm NP} \neq 0$, mainly due to two choices. First, the choice of narrow or wide bins for large-recoil $B \to K^*\mu\mu$ has an impact to the sensitivity to $\mathcal{C}_{9'}^{\rm NP}$: P_5' has a sensitivity to $\mathcal{C}_{9'}^{\rm NP}$ through its q^2-dependence at large recoil, which is probed if one chooses three narrow bins, but not if only one wide bin is considered. Taking narrow bins for $B \to K^*\mu\mu$ induced thus a tension between $P_5'(B \to K^*\mu\mu)$, which favours $\mathcal{C}_{9'}^{\rm NP} < 0$, and $Br(B \to K\mu\mu)$ at low-recoil, which favoured $\mathcal{C}_{9'}^{\rm NP} > 0$. Second, the need for $\mathcal{C}_{9'}^{\rm NP} > 0$ stemmed from the inclusion of $Br(B \to K\mu\mu)$. The presence of a significant resonant structure $\psi(4160)$ in the first low-recoil bin requires one to understand better the range of validity of Operator Product Expansion and quark-hadron duality to deal with resonant structures and predict observables at low recoil. Moreover, it turns out that new results presented by LHCb at this conference with very fine binning [5] indicate a branching ratio lower than SM expectations. Such low branching ratio agrees with a scenario where $\mathcal{C}_9^{\rm NP} < 0$ and $\mathcal{C}_{9'}^{\rm NP} = 0$. In other words, the constraint from $Br(B \to K\mu\mu)$ shown on the left panel of fig. 5 should go down with the new result from LHCb, pushing the global fit results much closer to the axis $\mathcal{C}_{9'}^{\rm NP} = 0$, in better agreement with the analysis presented above [1].

5 Limitations and prospects

If all the analyses point towards the need for a value of $\mathcal{C}_9$ differing from the Standard Model, there are several issues to be dealt with before claiming the presence of New Physics. The first is the possibility of a statistical fluctuation in $B \to K^*\mu\mu$ data. This can be tested thanks to a redundancy in the angular coefficients measured. Indeed, in the absence of new CP-violation in the Wilson coefficients, and negligible $P_{3,5',8'}$, one can derive a relation between $P_{1,2,4',5'}$, which provides an interesting consistency relation between the various measurements [15]. The above formula would be fulfilled to a better accuracy if the third bin for P_5' goes down (closer to SM) and the third bin for P_2 goes up (away from the SM). One thus can expect further changes in $B \to K^*\mu\mu$ data, but it is unlikely that this will bring all observables closer to SM.

On the theoretical side, an important issue comes from $c\bar{c}$ loops, which contribute to $\mathcal{C}_9$. The first contribution comes from charmonium resonances: at large recoil, the bins for $q^2 \leq 6$ GeV^2 are expected to be little affected by the J/ψ tail, whereas the predictions at low recoil hinge on the use of quark-hadron duality. The accuracy of the latter is expected to be of a few percent for the branching ratio, but has still to be assessed for other observables [16]. Moreover the model used to estimate the violations has to be updated to include the resonance observed by LHCb in the $B \to K\ell\ell$ channel. Another contribution comes from the non-resonant continuum, already included at leading order through $Y(q^2)$. The contribution from hard gluons can be estimated perturbatively through an effective theory approach. At large recoil, the contribution from soft gluons is supposed to be included through Operator Product Expansion and quark-hadron duality at low recoil. First results based on LCSR indicate that the contribution from soft gluons for $B \to K^*\ell\ell$ is positive, tending to increase the size of $\mathcal{C}_9^{\rm NP} < 0$ to reproduce the data at large recoil. However, a parallel with the $B \to K\ell\ell$ case suggests that this result could be modified significantly by additional contributions not considered in this first estimate [7,17].

A different issue on the theoretical side consists in the assessment of power-suppressed corrections for the predictions of exclusive decays. The computation of the transversity amplitudes in effective approaches does not involve only the translation of full form factors into soft form factors (factorisable corrections) but also additional contributions at the level of the amplitudes (non-factorisable corrections). These non-factorisable corrections yield further perturbative and non-perturbative corrections (from QCD factorisation at large K^* recoil and from Operator Product Expansion at low K^* recoil). Most of the analysis have seen no need for large contributions from these power-suppressed corrections, both at the factorisable and non-factorisable levels. A comparison of several models of form factors has led to recent claims [18] that such large factorisable power-corrections would be needed, leading to a significant increase in the uncertainties on the predictions of $B \to K(^*)\ell\ell$ observables at large recoil, but this claim has to be confirmed by further analyses of these power corrections.

It appears thus that more thorough theoretical work is needed to elucidate SM long-distance contributions to exclusive $b \to s$ transitions, to refine the predictions of form factors and to assess the limits of quark-hadron duality hypothesis, whereas a considerable experimental improvement would consist in having narrower bins for $B \to K^*\ell\ell$ similarly to what has been presented by LHCb at this conference. The combination of all these elements would yield a more accurate determination of Wilson coefficients in the effective Hamiltonian approach, providing valuable inputs for NP models aiming at reproducing the deviations observed in the $b \to s$ radiative transitions [5].

References

1. S. Descotes-Genon, J. Matias and J. Virto, Phys. Rev. D **88** (2013) 074002 [arXiv:1307.5683 [hep-ph]].
2. W. Altmannshofer and D. M. Straub, Eur. Phys. J. C **73** (2013) 2646 [arXiv:1308.1501 [hep-ph]].
3. F. Beaujean, C. Bobeth and D. van Dyk, arXiv:1310.2478 [hep-ph].
4. R. R. Horgan, Z. Liu, S. Meinel and M. Wingate, arXiv:1310.3887 [hep-ph], and Phys. Rev. D **89** (2014) 094501 [arXiv:1310.3722 [hep-lat]].
5. M. Pattel, E. Ben-Haïm, M. Gorbahn, Ch. Bobeth, W. Altmanshoffer, this conference.
6. P. Ball and R. Zwicky, Phys. Rev. D **71** (2005) 014029 [hep-ph/0412079].
7. A. Khodjamirian, T. .Mannel, A. A. Pivovarov and Y. -M. Wang, JHEP **1009** (2010) 089 [arXiv:1006.4945 [hep-ph]].
8. S. Descotes-Genon, J. Matias, M. Ramon and J. Virto, JHEP **1301** (2013) 048 [arXiv:1207.2753 [hep-ph]].
9. J. Matias, F. Mescia, M. Ramon and J. Virto, JHEP **1204** (2012) 104 [arXiv:1202.4266 [hep-ph]].
10. C. Bobeth, G. Hiller and D. van Dyk, JHEP **1007** (2010) 098 [arXiv:1006.5013 [hep-ph]].
11. S. Descotes-Genon, T. Hurth, J. Matias and J. Virto, JHEP **1305** (2013) 137 [arXiv:1303.5794 [hep-ph]].
12. C. Bobeth, G. Hiller and D. van Dyk, Phys. Rev. D **87** (2013) 034016 [arXiv:1212.2321 [hep-ph]].
13. RAaij *et al.* [LHCb Collaboration], Phys. Rev. Lett. **111** (2013) 191801 [arXiv:1308.1707 [hep-ex]].
14. S. Descotes-Genon, D. Ghosh, J. Matias and M. Ramon, JHEP **1106** (2011) 099 [arXiv:1104.3342 [hep-ph]].
15. J. Matias and N. Serra, arXiv:1402.6855 [hep-ph].
16. M. Beylich, G. Buchalla and T. Feldmann, Eur. Phys. J. C **71** (2011) 1635 [arXiv:1101.5118 [hep-ph]].
17. A. Khodjamirian, T. .Mannel and Y. M. Wang, JHEP **1302** (2013) 010 [arXiv:1211.0234 [hep-ph]].
18. S. Jäger and J. Martin Camalich, JHEP **1305** (2013) 043 [arXiv:1212.2263 [hep-ph]].